SUPPLEMENTAL FIGURES

Aberrant homeodomain-DNA cooperative dimerization underlies distinct developmental defects in two dominant *CRX* retinopathy models

Authors

Yiqiao Zheng[1,2,§], Gary D. Stormo[4*], Shiming Chen[2,3*]

Affiliations

[1] Molecular Genetics and Genomics Graduate Program, Division of Biological and Biomedical Sciences [2] Department of Ophthalmology and Visual Sciences [3] Department of Developmental Biology [4] Department of Genetics, Washington University in St Louis, Saint Louis, Missouri, 63110, USA [§] Current address: Department of Biology, Massachusetts Institute of Technology

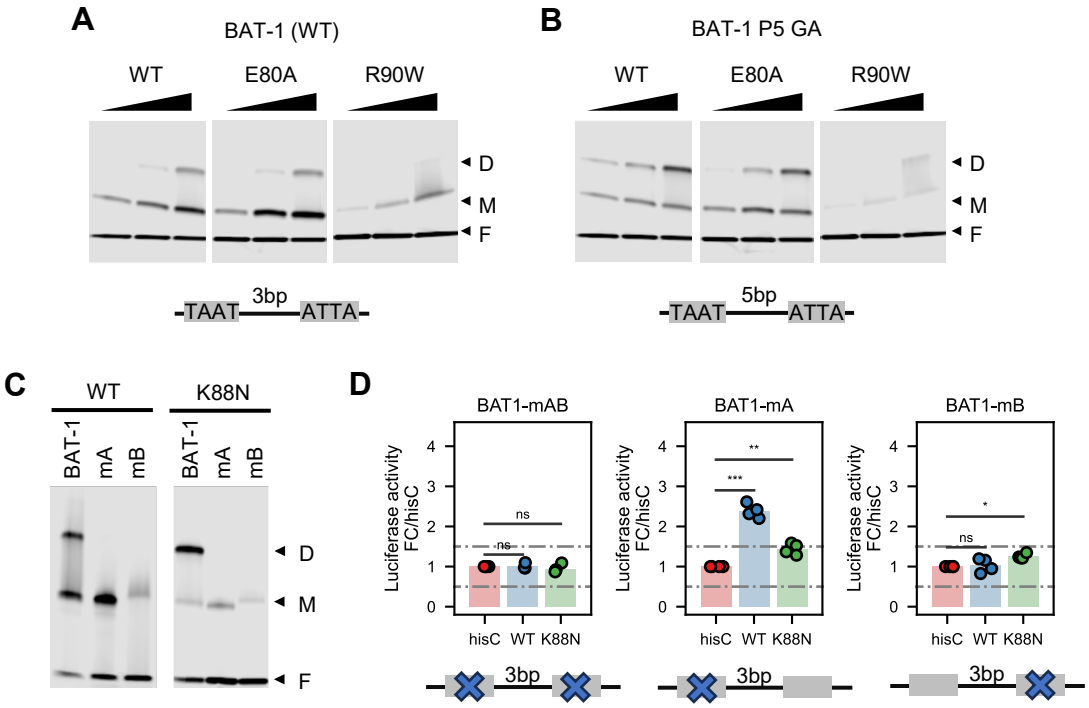

Supplemental Fig S1

Supplemental Fig S1 – P3 configuration and intact half-sites are required for K88N HD cooperative binding and transactivation activity. (*A,B*) EMSA gel images showing increasing amounts of WT, E80A, and R90W HD peptides bound to a fixed amount of BAT-1 (WT) or P5 probes. The cartoon underneath each gel image shows the dimeric HD motif configuration and is labeled with the spacer length. Note the WT HD EMSA gel images are the same as in Fig. 1C,D. (*C*) EMSA gel images showing WT and K88N HD peptides bound to BAT-1 (WT), mA and mB probes. (*D*) Barcharts of luciferase reporter assays comparing CRX WT and K88N transactivation activity at BAT-1 variant enhancer sequences. The cartoon underneath each barchart shows the HD core motif mutated. Bars represent the mean. *p-values* of one-way ANOVA are annotated: ns: >5e-2; *: <=5e-2; **: <=1e-2; ***: <=1e-3.

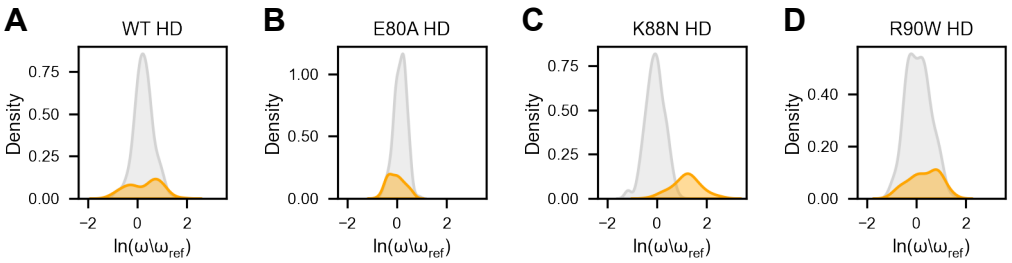

Supplemental Fig S2

Supplemental Fig S2 – WT and mutant CRX HDs demonstrate similar cooperativity profiles at P5 library but distinct cooperativity profiles at P3 library. (*A-D*) Histograms depicting the distribution of CRX HD relative cooperativity on members of the P5 library (grey) and the P3 library (orange). Relative cooperativity against the reference sequence TAATGCGCTATTA is plotted (ω/ω_{ref}). Note the relative cooperativity is presented in the Logarithmic scale. The full relative cooperativity matrix can be found in Supplemental Table S2.

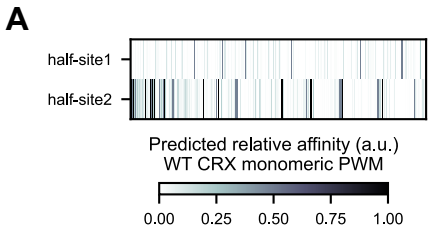
A
half-site1
half-site2
Predicted relative affinity (a.u.)
WT CRX monomeric PWM
0.00
0.25
0.50
0.75
1.00

Supplemental Fig S3 – Dimeric K_{50} HD motifs in *Crx*$^{E80A/A}$-reduced ATAC-seq peaks composed of low-affinity half-sites. (*A*) Heatmap depicting the predicted half-site affinity of FIMO-found dimeric K_{50} HD motifs under *Crx*$^{E80A/A}$-reduced ATAC-seq peaks. The dimeric motifs are ordered by FIMO p-values. The half-site relative affinity, normalized to consensus TAATCC, is predicted using the published WT CRX PWM model (Supplemental Table S4; Methods).

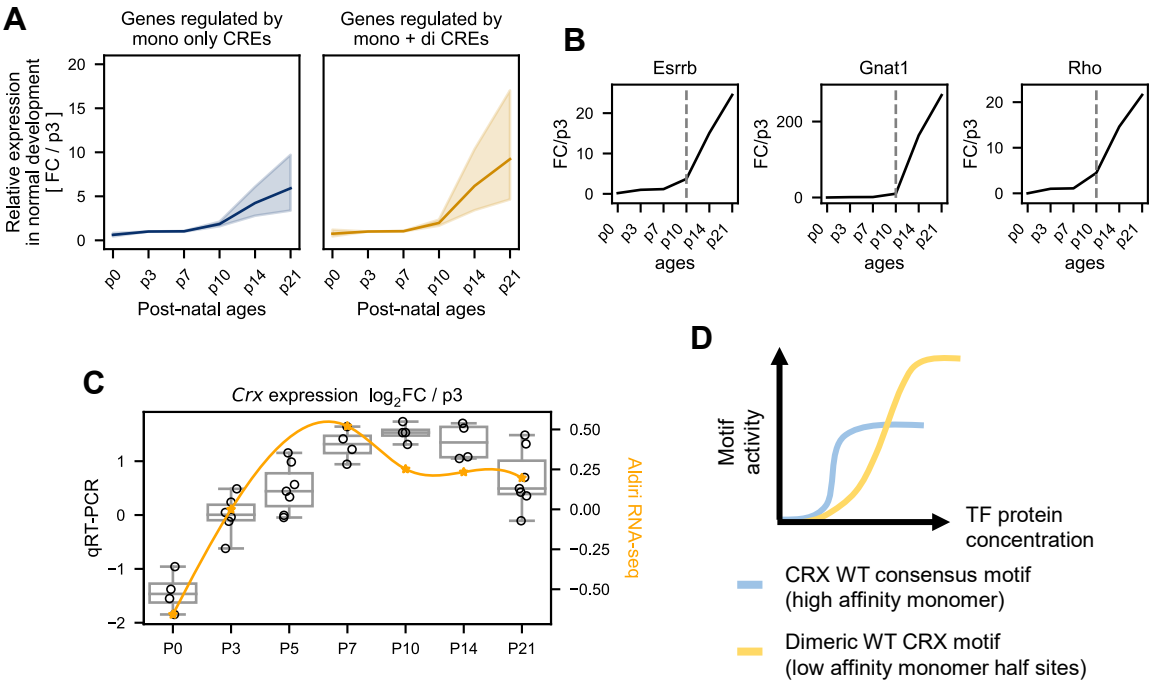

Supplemental Fig S4

Supplemental Fig S4 – Dimeric K_{50} HD motifs are associated with stage-specific gene regulation. (*A*) Line plots showing the expression dynamics of genes associated with CREs with only monomeric or both monomeric and dimeric K_{50} HD motifs. Expression levels are normalized to P3 and represented by fold-change. (*B)* Expression line plots of selected genes associated with monomeric and dimeric K_{50} HD motifs. (*C*) Dual-axes box and line plot showing the *Crx* mRNA developmental expression patterns measured by qRT-PCR (left axis, box and strip plot) and by whole-retina RNA-seq (right axis, line and scatter plot). Expression levels are normalized to post-natal day 3 (P3) and presented by log-fold-change. The developmental RNA-seq data in Supplemental Fig**.** S4A-S4C is from Aldiri et al. 2017. (*D*) Diagram depicting the stage-specific activity model of CRX WT high-affinity monomeric motifs and dimeric motifs with individually low-affinity half-sites.

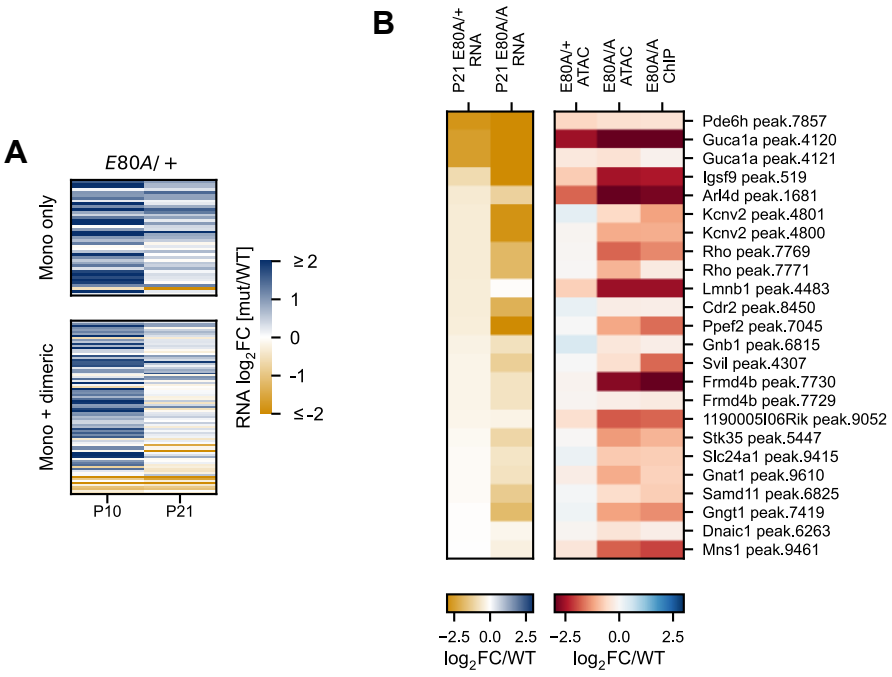

Supplemental Fig S5

Supplemental Fig S5 – CRX-DAGs regulated by dimeric K_{50} HD motifs are selectively down-regulated in *Crx^{E80A}* mutant retinas. (*A*) Heatmap comparing the CRX-DAG expression changes in the *Crx$^{E80A/+}$* retinas at ages of post-natal day 10 (P10) and day 21 (P21). The gene sets in the heatmaps are as defined in Fig. 6A. The order of the genes is identical to that in Fig. 6B. (*B*) Heatmaps showing down-regulated genes with correspondingly decreased chromatin accessibility at associated CREs in the *Crx^{E80A}* retinas. The genes and CREs are ordered first by RNA-seq logFC than by ATAC-seq logFC in the *Crx$^{E80A/A}$* retinas. The peak.id denotes the unique CRX ChIP-seq peak associated with a gene. The full CRX bound CRE-gene association matrix can be found at Supplemental Table S6.

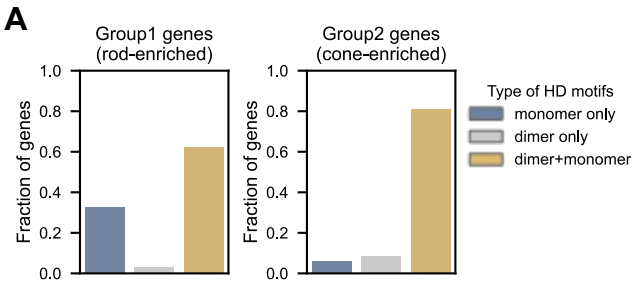
A
Group1 genes
(rod-enriched)
Group2 genes
(cone-enriched)
Fraction of genes
1.0
0.8
0.6
0.4
0.2
0.0
Type of HD motifs
monomer only
dimer only
dimer+monomer

Supplemental Fig S6 – Dimeric K_{50} HD motifs are associated with cell type-specific gene regulation. (*A*) Barcharts showing the distribution of cone- vs rod-enriched CRX-DAGs associated with CREs containing monomeric, dimeric, or both types of K_{50} HD motifs. The definition of Group1 and 2 genes is taken directly from our previous publication Zheng et al. 2023.

A

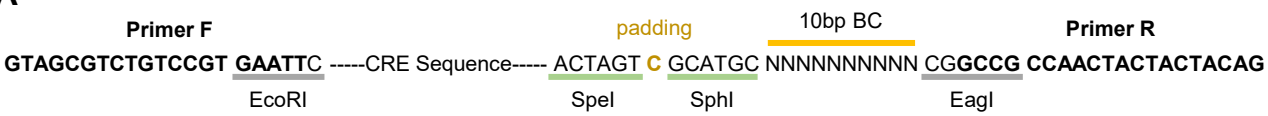

B

	Category	N	Include in MPRA lib	HD site mutants	# BC/CRE	Total testing CREs
1	K88N/N gained	466	1031	1440	4	9884
2	E80A/A gained	214			4	
3	E80A/A lost	309			4	
4	CREs for selected genes	55			4	
5	Rest of ChIP peaks not in categories 1-4 (expected)	8798	900	799	4	6796
6	Basal		1		20	20
7	Scrambles		150		4	600
8	+ Ctrl		20		6	120
	TOTAL		4345			17420

Supplemental Fig S7

Supplemental Fig S7 – MPRA oligo design and library composition. (*A*) Diagram of a typical testing MPRA oligo. The restriction enzyme cut sites used for cloning, primer sites for amplification, and testing CRE and barcode locations are noted. (*B*) Table displaying the composition of MPRA library designed and ordered. The gained and lost categories were defined by comparing the ChIP-seq signal intensity (Methods; MPRA GitHub repository).